DIRAC note 10-02

Calibration of Ionization Hodoscope for 2008 runs

Jan Smolík[1,2] and Valeriy Yazkov[3]

[1] *Czech Technical Univesity, Prague*
[2] *Instute of Physic, ASCR, Prague*
[3] *SINP, Moscow*

June 29, 2010

Abstract

The calibration procedure for single hit amplitude of individual slabs of Ionisation Hodoscope is described here. The results for 2008 runs are briefly presented.

Introduction

The Ionisation Hodoscope (IH) serves among other things as a complementary detector to Scintillation Fibre Detector (SFD). It allows to distinguish two very close hits from one hit using amplitude information from IH. The design of IH and its characteristics are described in detail in [1]. It consists of four planes of size $11x11cm^2$. Each plane is formed from sixteen scintillating slabs of $11cm$ length $7mm$ wide and $1mm$ thick. The slabs are connected to PMT's through light guides of different lengths. The slabs in the first and the third plane are oriented in X direction (X1 and X2) and in other two planes in Y direction (Y1 and Y2). The planes with the same orientation are shifted of half of slab width to respect to each other to cover dead space between slabs.

As already observed in [1] the single hit amplitudes depend on longitudinal position of hit in slab and their average values can change in time. Moreover due to long operation time the measured longitudinal characteristic can change. Therefore the study of longitudinal dependence of single hit amplitude was repeated for 2008 data sample.

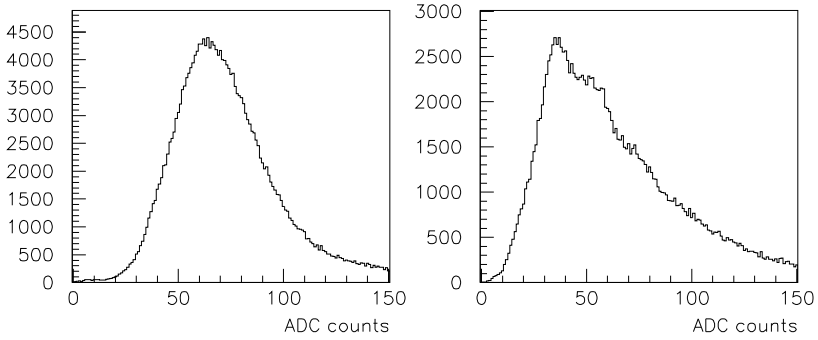

Figure 1: Illustration of single hit spectra. On the left typical shape of slab with weak longitudinal dependences (the 10^{th} slab of the 2^{nd} plane). On the right spectrum of slab with strong longitudinal dependence (the 6^{th} slab of the 4^{th} plane)

1 Event selection

As the analyses is aimed to study single hit amplitude position the appropriated selection criteria to minimalize number of double hits was chosen. We accepted only 'good' events with standard pion trigger and two reconstructed tracks - one per arm. Around the corresponding hits in SFD in region ± 20 fibres we demand no another hits. To decrease background from proton we choose only hits corresponding to negative tracks.

The selection criteria significantly decrease the statistic. To have enough events in reference sample we found interval of runs where the average value of single-hit amplitudes is more or less stable. The select interval consists of all standard runs from run number 8405 to 8495 except 8437,8453,8464,8466,8474-8476,8482,8488 and 8489. For illustration two spectra are shown on Figure 1.

2 Longitudinal dependence of amplitude

Due to long and narrow shape of slabs the amplitude depends on longitudinal position of hit. Different length of light guides and aging effects causes that the longitudinal dependence differs slab to slab.

To study the longitudinal dependence each slab were divided into twelve section with 1cm of length (two outer section cover only $\sim$ .5cm of scintillator). For each section we found position of single-hit amplitude peak using Gaussian approximation of the top of the peak. The longitudinal dependence given by the position of the peaks in twelve section was fit using polynomial approximation. The fourth order polynomial seems to be sufficient (exact form was like in [1])

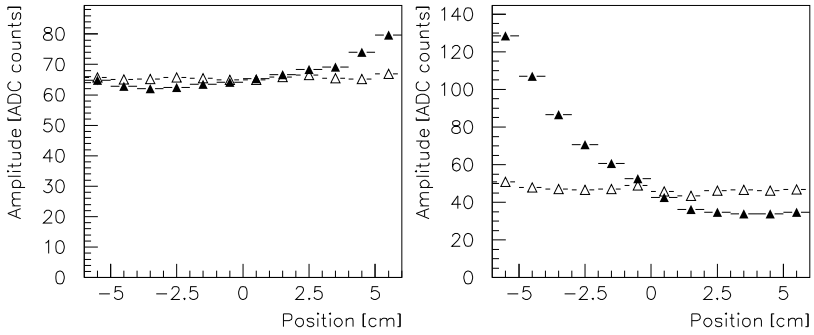

Figure 2: Longitudinal dependence of single-hit amplitude. Left -the 10^{th} slab of the 2^{nd} plane, Right - the 6^{th} slab of the 4^{th}th plane of IH. The filled triangles correspond to raw amplitudes, the blank triangles correspond to amplitudes weighted by $A(0)/A(y)$.

$$A(y) = A(0)Y(y) = A(0)(1 + y(c_1 + y(c_2 + y(c_3 + yc_4)))) \tag{1}$$

Two illustrative dependences are shown at Figure 2. The results of the procedure are summarised in Table 1. The most of slabs show relatively weak dependence but for several slabs it is violent.

To test significance of longitudinal dependence we compare RMS of spectrum of raw amplitude over all slab with weighted one. As weight we use function $A(0)/A(y)$. RMS was evaluated in region of ± 2.5 RMS around the centre of the peak. The peak positions and RMS of both spectra and the ration of RMS are shown in Table 2. It can be seen, that the weighted spectra have slightly shifted position of peak and smaller RMS to compare with raw ones. The ration of RMS vary from 1. to 0.5, for most of slab is higher than 0.9. The values of amplitudes are in ADC channel count after pedestal subtraction

3 Time Dependence

The average values of single-hit amplitudes can vary run to run. Therefore we study position of single-hit peak for each run. We suppose that the shape of the longitudinal dependence is time-independent during 2008 seance and only value of $A(0)$ in 1 changes in time. For each run the weighted spectra (weighed by $A(0)/A(y)$) were constructed and fitted by Gauss function to find peak position. The extracted time dependence is demonstrated in Figure 3. For most of slabs and runs the variation of peak position is in 15% range.

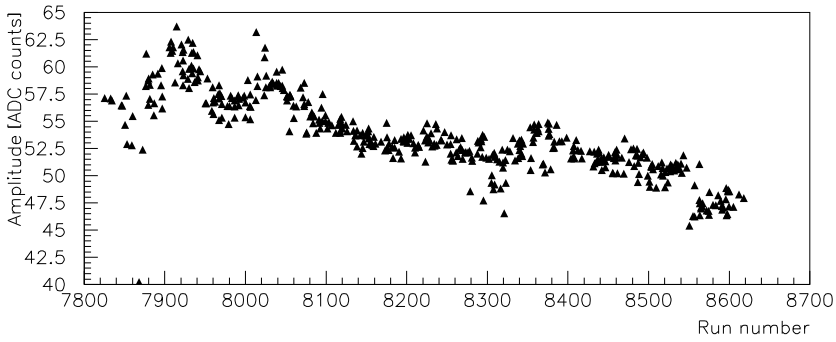

Figure 3: Time dependence of single-hit amplitude peak position for 7th slab of the 1st plane of IH during 2008 seance. The position of peak is shown in ADC channels after pedestal subtraction.

4 Conclusion

The longitudinal and position dependence of single-hit amplitude of Ionisation Hodoscope was studied. The improvements of width of spectrum reach by introducing correction on longitudinal dependence is about 10% for most of slabs. The variation of peak varied mostly in 15% range during 2008 running period.

The estimation of number of photoelectrons for each slab was done and the results are shown in Table 3.

References

[1] V.Brekhovskikh at. al.,DIRAC NOTE 2002-09

Plane	Slab	A(0)	c(1)	c(2)	c(3)	c(4)
1	1	56.0372	7.31E-03	6.76E-04	1.14E-04	7.25E-05
1	2	59.7542	1.45E-02	8.76E-05	-4.00E-04	1.39E-04
1	3	61.7700	2.32E-02	3.68E-03	5.08E-04	1.56E-04
1	4	53.9033	4.27E-02	8.51E-03	7.75E-04	-5.91E-05
1	5	51.8279	2.13E-02	2.10E-03	4.11E-04	6.24E-05
1	6	56.0430	2.24E-02	2.82E-03	2.99E-04	1.45E-04
1	7	51.7819	1.09E-02	2.09E-03	4.10E-04	5.36E-05
1	8	49.2752	1.16E-02	1.85E-03	7.36E-04	1.43E-04
1	9	65.2669	4.72E-02	7.78E-04	1.10E-03	4.24E-04
1	10	60.5431	3.10E-02	2.38E-03	-9.15E-05	5.06E-05
1	11	70.5067	2.28E-02	1.41E-03	2.23E-04	1.02E-04
1	12	60.9333	1.28E-02	-3.71E-04	-4.85E-04	1.43E-04
1	13	59.2625	2.08E-02	1.04E-03	2.68E-05	1.80E-04
1	14	63.0544	2.33E-02	4.62E-03	2.75E-03	5.21E-04
1	15	61.7938	1.78E-02	-1.14E-03	-2.11E-04	2.05E-04
1	16	61.7834	7.91E-03	2.91E-03	2.16E-04	0.00E+00
2	1	66.4344	2.64E-02	8.53E-06	-9.55E-05	1.62E-04
2	2	69.3362	1.63E-02	-1.96E-04	4.95E-04	2.18E-04
2	3	65.9775	1.41E-02	9.03E-04	3.79E-04	1.31E-04
2	4	68.2214	1.15E-02	1.15E-03	1.70E-04	4.40E-05
2	5	53.0497	3.08E-02	-1.00E-03	6.21E-04	3.88E-04
2	6	49.0640	1.37E-02	2.65E-04	9.61E-04	2.03E-04
2	7	62.0744	3.34E-03	-3.67E-03	1.41E-03	4.35E-04
2	8	69.9729	1.36E-02	9.17E-04	7.64E-05	4.97E-05
2	9	72.2146	4.05E-03	1.08E-03	5.24E-04	1.31E-04
2	10	64.8964	1.56E-02	-2.60E-04	1.37E-04	1.34E-04
2	11	56.1463	1.15E-02	-2.12E-03	5.63E-04	3.54E-04
2	12	57.3022	1.33E-02	8.64E-04	-9.73E-05	7.24E-05
2	13	64.0861	1.16E-02	1.27E-04	8.95E-05	1.20E-04
2	14	51.8176	1.58E-02	2.37E-03	3.40E-04	6.97E-05
2	15	51.3734	2.53E-03	5.54E-05	2.29E-04	6.09E-05
2	16	47.6843	1.71E-02	1.57E-03	6.69E-04	2.38E-04
3	1	57.8120	3.51E-02	1.28E-03	-5.90E-04	9.79E-05
3	2	53.0873	1.28E-02	-8.85E-04	-9.25E-05	1.26E-04
3	3	56.9952	1.91E-02	3.17E-03	3.15E-05	1.06E-04
3	4	64.4253	3.64E-02	6.35E-03	7.78E-04	1.42E-04
3	5	64.8835	1.29E-02	3.82E-03	4.01E-04	9.84E-05
3	6	54.3482	1.40E-02	3.02E-03	2.29E-04	0.00E+00
3	7	57.6340	1.02E-02	6.72E-05	-1.03E-04	1.27E-04
3	8	68.7494	1.52E-02	8.91E-04	2.40E-04	6.42E-05
3	9	59.7921	2.10E-02	2.04E-03	2.66E-04	6.63E-05
3	10	76.7616	9.19E-03	8.31E-04	1.64E-04	6.84E-05
3	11	55.5978	2.27E-02	2.25E-03	3.75E-04	1.49E-04
3	12	70.3643	2.97E-02	4.41E-03	0.00E+00	0.00E+00
3	13	67.5819	7.99E-03	1.13E-03	-3.25E-05	8.73E-05
3	14	68.5255	2.65E-02	1.18E-03	-8.99E-05	8.28E-05
3	15	81.7188	1.14E-02	1.15E-03	4.39E-04	1.30E-04
3	16	74.6613	1.63E-02	2.98E-03	0.00E+00	0.00E+00
4	1	39.0673	-8.18E-02	1.48E-02	-2.95E-03	4.23E-04
4	2	62.4821	-2.22E-02	-1.62E-04	-3.93E-04	1.43E-04
4	3	53.8776	-8.46E-02	2.94E-02	-2.98E-03	-6.75E-05
4	4	64.9586	-3.68E-02	-7.34E-03	-8.32E-04	3.49E-04
4	5	46.7486	-1.76E-02	-7.22E-04	-1.04E-03	2.92E-04
4	6	46.3033	-1.64E-01	2.51E-02	-3.89E-04	0.00E+00
4	7	70.0879	-4.35E-02	4.06E-03	0.00E+00	0.00E+00
4	8	67.5061	-1.43E-02	-1.22E-04	-3.70E-04	1.39E-04
4	9	55.8840	-1.42E-02	3.73E-03	-1.77E-03	3.40E-04
4	10	60.7629	-2.71E-02	2.89E-04	-1.18E-04	1.43E-04
4	11	63.0716	-1.38E-02	1.37E-03	-5.52E-04	1.39E-04
4	12	64.1221	-1.70E-02	2.23E-03	-1.30E-03	1.84E-04
4	13	49.7254	-1.88E-02	5.07E-04	-1.05E-03	2.52E-04
4	14	85.4571	-1.50E-02	1.44E-03	-4.41E-04	1.13E-04
4	15	52.2015	-1.69E-02	2.03E-03	-3.47E-04	1.15E-04
4	16	57.7772	-1.84E-02	-4.50E-03	-1.15E-03	5.65E-04

Table 1: The parameters of fitted longitudial dependence of single hit amplitude.

Plane	Slab	Mean	Mean-weigted	RMS	RMS-weigted	RMS ratio
1	1	59.59	58.64	14.87	14.48	0.974
1	2	63.35	62.72	14.53	14.05	0.967
1	3	67.74	65.31	17.26	15.48	0.897
1	4	59.55	56.58	18.18	15.32	0.843
1	5	55.44	54.33	15.29	14.48	0.947
1	6	60.41	58.26	14.45	13.02	0.901
1	7	55.31	53.99	14.21	13.61	0.958
1	8	53.20	51.45	14.70	13.82	0.940
1	9	71.49	69.75	23.25	20.01	0.861
1	10	64.20	62.67	15.79	14.55	0.921
1	11	75.47	74.19	18.89	17.73	0.939
1	12	64.30	63.77	15.39	15.14	0.983
1	13	64.05	62.38	17.95	16.99	0.947
1	14	70.95	66.62	23.10	19.29	0.835
1	15	65.85	64.78	17.24	16.78	0.973
1	16	65.33	64.00	14.12	13.55	0.960
2	1	71.25	69.92	17.92	16.74	0.934
2	2	74.13	72.02	17.92	16.69	0.931
2	3	70.78	68.98	17.51	16.39	0.936
2	4	72.44	71.51	17.24	16.58	0.962
2	5	58.12	56.70	18.69	16.93	0.906
2	6	53.50	52.08	17.75	16.97	0.956
2	7	67.02	65.54	19.56	18.52	0.947
2	8	73.88	73.01	16.76	16.28	0.971
2	9	77.78	76.57	19.53	18.85	0.965
2	10	69.62	68.86	20.02	19.53	0.976
2	11	60.13	59.13	16.25	15.46	0.951
2	12	60.45	59.81	14.43	13.98	0.969
2	13	67.95	67.07	15.92	15.45	0.971
2	14	55.31	54.23	14.10	13.32	0.945
2	15	54.98	54.79	17.21	17.21	1.000
2	16	51.92	50.44	14.64	13.33	0.911
3	1	61.42	60.11	14.87	13.86	0.932
3	2	55.43	55.28	13.82	13.75	0.995
3	3	61.98	60.63	17.54	16.77	0.956
3	4	71.44	67.98	21.71	19.41	0.894
3	5	70.37	68.42	18.06	16.95	0.939
3	6	57.15	55.8	13.08	12.68	0.969
3	7	61.48	60.49	16.98	16.62	0.979
3	8	73.51	72.87	19.74	19.23	0.974
3	9	63.24	62.53	15.33	14.54	0.948
3	10	81.51	80.23	19.71	19.38	0.983
3	11	59.30	57.47	14.66	13.69	0.933
3	12	76.13	74.37	19.77	18.46	0.934
3	13	71.65	70.85	16.81	16.37	0.974
3	14	72.59	71.66	17.25	16.38	0.950
3	15	87.24	85.83	21.43	20.71	0.967
3	16	78.84	77.06	15.09	14.35	0.951
4	1	47.18	41.81	18.97	13.97	0.737
4	2	66.32	64.95	15.35	14.25	0.928
4	3	66.44	57.44	24.85	15.30	0.616
4	4	67.58	67.42	17.57	15.00	0.854
4	5	50.29	48.73	13.39	12.03	0.898
4	6	57.93	48.92	26.31	14.81	0.563
4	7	77.41	74.12	22.45	19.92	0.887
4	8	71.82	69.99	15.98	15.13	0.946
4	9	62.99	59.20	18.63	16.17	0.868
4	10	65.22	63.32	17.35	16.14	0.930
4	11	67.26	64.88	14.12	12.81	0.907
4	12	70.98	68.49	21.42	19.33	0.903
4	13	53.86	52.26	14.78	13.39	0.906
4	14	92.14	89.74	20.97	19.25	0.918
4	15	56.31	54.57	14.61	13.65	0.934
4	16	62.74	60.69	16.72	14.85	0.888

Table 2: Comparation of mean and rms of raw and weighted single hit spectra. The RMS is computedin interval $\pm 2.5 RMS$ around mean

	Plane			
Slab	1	2	3	4
1	12.9	20.6	18.5	9.4
2	20.8	15.8	14.9	20.6
3	16.3	14.3	13.0	16.0
4	9.7	17.9	10.7	21.3
5	13.4	10.0	16.9	14.1
6	16.2	7.6	20.9	10.3
7	14.7	10.6	13.3	11.2
8	12.7	19.2	15.0	20.0
9	11.9	14.0	20.5	12.3
10	17.7	12.8	14.5	12.9
11	16.4	13.6	16.7	25.0
12	19.2	17.8	15.7	11.0
13	14.3	20.8	19.7	13.7
14	11.2	16.0	17.9	26.0
15	14.7	8.4	16.9	15.5
16	20.5	16.2	37.9	18.2

Table 3: Aproximate numbers of photoelectrons obtained as a square of ration of position and width of amplitude peaks.